View metadata, citation and similar papers at core.ac.uk
brought to you by CORE
provided by KnowledgeBank at OSU

Experimental Confirmation of Quantum Monodromy: The Millimeter Wave Spectrum of Cyanogen Isothiocyanate NCNCS

Brenda P. Winnewisser, Manfred Winnewisser, Ivan R. Medvedev, Markus Behnke, and Frank C. De Lucia
Department of Physics, The Ohio State University, Columbus, Ohio 43210-1106, USA

Stephen C. Ross
Department of Physics and Centre for Laser, Atomic, and Molecular Sciences, University of New Brunswick, P.O. Box 4400, Fredericton, New Brunswick E3B 5A3, Canada

Jacek Koput
Department of Chemistry, Adam Mickiewicz University, 60-780 Poznan, Poland
(Received 22 August 2005; published 5 December 2005)

We have made energy-momentum maps for the experimental end-over-end rotational energy and the two-dimensional bending vibrational energy, both of which confirm the dominating effects of nontrivial quantum monodromy in cyanogen isothiocyanate. Accidental resonances in the rotational spectra yield accurate intervals between bending states.

DOI: 10.1103/PhysRevLett.95.243002 PACS numbers: 31.15.Ar, 31.50.Bc, 33.15.Hp, 33.20.Bx

The concept of monodromy (Greek for "once around") in a champagne bottle potential was introduced in 1991 by Bates [1]. For a two-dimensional anharmonic oscillator with a potential function resembling the bottom of a champagne bottle, the hump represents a "gross topological obstruction." The top of the barrier is called the critical or monodromy point. Child and collaborators [2–4] have translated the abstract mathematics into the language of quantum mechanics and spectroscopy. They pointed out via classical trajectory calculations that the sense of precession for a particle changes sign abruptly if the trajectory moves from below the monodromy point to above the monodromy point.

In search of a molecule with an isotropic two-dimensional anharmonic potential function with more than one bending state below its monodromy point we rediscovered cyanogen isothiocyanate, NCNCS, the microwave spectrum of which was measured and partially assigned in a masterful analysis by King, Kroto, and Landsberg in 1985 [5]. The central bending potential function was shown from the initial analysis of the microwave data to have a barrier height to linearity of about 270 cm^{-1} [6] with a low-lying bending mode around 90 cm^{-1}. This implies that we should be able to probe rovibrational energy states both below and above the monodromy point.

The r_e structure was calculated according to the coupled-cluster single double (triple) [CCSD(T)] and correlation-consistent polarized valence quintuple zeta [cc − pV(5 + *d*)Z] level of theory with corrections for the core-correlation effects at the CCSD(T)/cc − pCV(Q + d)Z level. The structure, displayed in Fig. 1, shows a planar chainform molecule. The components of the permanent electric dipole moment at this configuration are calculated at the CCSD(T)/cc − pV(Q + d)Z level to be $\mu_a = 3.20$ D and $\mu_b = 0.41$ D.

The fundamental vibrational wave numbers for NCNCS, which has molecular symmetry C_s, are given in Table I. The harmonic wave numbers were calculated at the CCSD(T)/cc − pV(T + d)Z level of theory. Anharmonic corrections calculated at the MP2/cc − pV(T + d)Z level of theory were added to yield the anharmonic wave numbers. The large amplitude bending motion, as can be seen from Fig. 1 and Table I, takes place about the central N atom.

Following the method of King and Kroto [7] the sample of NCNCS was prepared by the pyrolytic isomerization reaction of $S(CN)_2$ vapor in a flow system directly attached to the absorption cell at a pressure of 5 mTorr.

The spectroscopic measurements were carried out in the frequency range from 115 to 365 GHz using the fast scan submillimeter spectroscopic technique incorporating recent improvements [8,9]. The accuracy of the absorption line positions is estimated the be ±50 kHz.

The present data set contains rotational transitions arising from NCNCS molecules in the ground vibrational state and 5 excited bending states of the ν_7 mode, which we label ν_b indicating the use of bent (*b*) notation while ν_l will refer to linear (*l*) notation. As we shall see, both notations

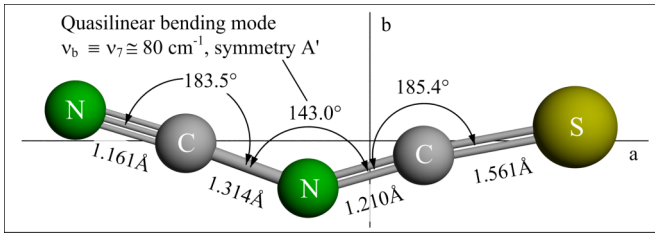

FIG. 1 (color online). *Ab initio* predicted equilibrium structure of NCNCS.

 © 2005 The American Physical Society

TABLE I. *Ab initio* predicted harmonic and anharmonic fundamental vibrational modes for NCNCS (Symmetry C_s).

	Γ	ω^a	ν^a	Harmonic potential energy distribution [N(1)C(2)N(3)C(4)S(5)]
ν_1	A'	2302	2258	73% 1–2 s^b, 22% 2–3 s
ν_2	A'	2058	2024	74% 3–4 s, 15% 4–5 s, 10% 1–2 s
ν_3	A'	1188	1178	47% 2–3 s, 41% 4–5 s, 13% 1–2 s
ν_4	A'	688	662	39% 4–5 s, 31% 2–3 s, 25% 3–4 s
ν_5	A'	483	472	68% 3–4–5 b, 19% 1–2–3 b, 11% 2–3–4 b
ν_8	A''	452	454	65% 2–3–4–5 t, 35% 1–2–3–4 t
ν_6	A'	444	447	74% 1–2–3 b, 25% 3–4–5 b
ν_9	A''	430	429	65% 1–2–3–4 t, 35% 2–3–4–5 t
ν_7	A'	89	80	94% 2–3–4 large amplitude bend

[a] ω stands for harmonic wave number in cm^{-1}, ν for anharmonic wave number in cm^{-1}.
[b] s stands for stretching, b for bending, t for torsional vibration.

are applicable to the vibrational eigenstates of NCNCS; the vibrational quantum number v_l is related to v_b via the relation $v_l = 2v_b + |K_a|$. The asymmetric rotor angular momentum quantum number K_a, the projection of the total angular momentum **J** on the axis of least moment of inertia, a, is identical with $|\ell|$ in the linear molecular model.

All rotational transitions discussed here were assigned to their respective J values using the Loomis-Wood option of the CAAARS assignment package [9] and adjusting the coefficients in a conventional power series in $J(J+1)$ for each value of v_b and K_a. The effective rotational constant B_{eff} multiplies the leading term $J(J+1)$ in each polynomial, representing the dominant contribution to the end-over-end rotation [$B_{\text{eff}} \approx (B+C)/2$ for a bent molecule, B for a linear molecule]. Assignments of K_a were obtained by combining the information from the microwave study [5] and predictions from the general semi-rigid bender (GSRB) Hamiltonian calculations [6]. Furthermore, line intensities and asymmetry (or ℓ-type doubling) splittings for $K_a = 1$, 2, and 3 were essential.

The key features of the GSRB [6,10] Hamiltonian are a kinetic energy representation of rotation and the large amplitude bend, and a semi-rigid contribution, allowing for the dependence of internuclear distances and end bond angles on the large amplitude bending coordinate. Only atomic masses are fixed; good starting values for the internuclear distances and end angles and for the bending potential function parameters are required. The structural and potential parameters and semirigidity parameters are adjusted in a fit to pure rotational or rovibrational data. For a detailed discussion the reader is referred to Refs. [6,11].

The map of end-over-end rotational energy, represented by B_{eff}, versus the angular momentum quantum number $\pm K_a$ (K_a is used here as in the classical sense), given in Fig. 2, displays the consequences of quantum monodromy in NCNCS. The experimental ΔB_{eff} values are listed in Table II. (The values for asymmetry doublets are averaged.) From the dependence of the B_{eff} values on v_b and K_a, it is obvious that neither the Hamiltonian for an asymmetric rotor molecule nor the Hamiltonian for a linear molecule is applicable over the entire range.

The available data for NCNCS includes no experimental $E(K_a, v_b)$ values. However, the GSRB Hamiltonian [11] allowed us to calculate the vibrational energy levels associated with the quasilinear bending mode ν_b given in Table III and thus to plot the graph for NCNCS shown in Fig. 3. This plot has precisely the topology predicted in the work of Bates [1] and Child [3] for a system with monodromy: The smooth, parabolic (blue online) curves in Fig. 3 representing the states $v_b = 0, 1, 2$, evolve rapidly to a succession of curves with sharp kinks at $K_a = 0$ beginning with the monodromy point at $v_b = 3$.

A quantitative confirmation of the accuracy of the GSRB predictions is provided by several local resonances observed in the pure rotational spectrum. For example, as indicated in Fig. 3, a $\Delta v_b = +1$, $\Delta K_a = -3$ local Coriolis resonance interaction has been observed around $J = 80$ between the bending states $v_b = 2$, $K_a = 4^e$ and $v_b = 3$, $K_a = 1^e$. The superscript ^{e} designates the parity. Though separated by about 5 cm^{-1} at low J, the two series of levels

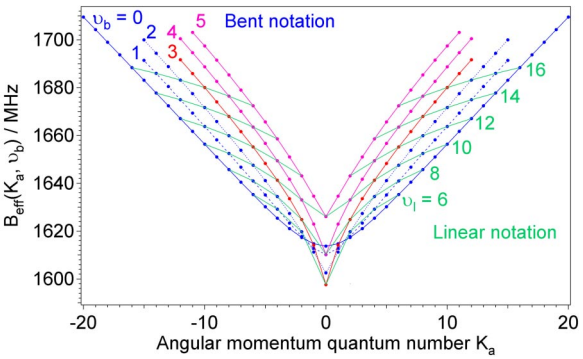

FIG. 2 (color online). Experimentally determined B_{eff} values for NCNCS plotted versus K_a.

TABLE II. Experimentally determined differences in rotational constants ΔB_{eff} in MHz for NCNCS. $\Delta B_{\text{eff}} = [B_{\text{eff}}(K_a, v_b) - B_{\text{eff}}(0,0)]$ with $B_{\text{eff}}(0,0) = 1613.7186$ MHz.

K_a	$v_b = 0$	$v_b = 1$	$v_b = 2$	$v_b = 3$	$v_b = 4$	$v_b = 5$
0	0.0000	−3.5075	−11.1772	−16.1337	−3.4351	12.3032
1	0.9807	−0.8821	−2.4494	0.3744	9.2121	20.8636
2	3.6019	4.0253	6.0088	11.1143	19.3301	29.3654
3	7.3238	9.6602	13.6557	19.8371	27.9588	37.2838
4	11.7077	15.4394	20.7407	27.5632	35.7309	44.8478
5	16.4984	21.3595	27.4372	34.5905	42.9530	51.9393
6	21.5298	27.2128	33.8673	41.4517	49.7988	58.7228
7	26.7094	32.9975	40.0970	47.9303	56.3726	65.2702
8	31.9818	38.7398	46.1747	54.2069	62.7267	71.6465
9	37.2949	44.4310	52.1315	60.3218	68.9231	77.8242
10	42.6339	50.0758	57.9895	66.3108	74.9724	83.7249
11	47.9872	55.6757	63.7636	72.1985	80.8818	89.3891
12	53.3404	61.2335	69.4709	77.9984	86.7637	
13	58.6910	66.7533	75.1110			
14	64.0313	72.2374	80.7062			
15	69.3616	77.6932	86.2514			
16	74.6778					
17	79.9810					
18	85.2724					
19	90.5513					
20	95.8181					

come to coincide at $J = 80$ because of differing B_{eff} values. A preliminary analysis shows that the values in Table III are accurate to better than 1 cm^{-1}. The evaluation of more of these resonances will allow a further refinement of the GSRB calculation.

Using the information describing the potential function derived from the GSRB for the quasilinear bending mode of NCNCS we obtain Fig. 4. This figure shows that the $K_a = 0$ level of the $v_b = 3$ state is just barely above the classical monodromy point.

Figure 2 reveals that NCNCS molecules in the $K_a = 0$ level of the $v_b = 3$ state feature the smallest effective rotational constant and therefore the largest moment of inertia. This effect was observed for the first time during the analysis of CH_3NCS [12,13] a quasisymmetric top, which actually has two states below the monodromy point, and again in the quasilinear molecules BrCNO and ClCNO [11], both of which have one $K_a = 0$ state well below the monodromy point. In the case of all of these molecules, the pronounced drop in B-value for low K_a values near the top of the barrier is the result of the quantum mechanical or classical time average of the moment of inertia. This effect is most clearly seen to be systematic in the case of NCNCS.

The topology of the bending potential function is indeed distinctively mapped onto the observed spectrum and thus

TABLE III. Calculated term values $E(K_a, v_b)/hc$ in cm^{-1} for the large amplitude bending mode ν_b of NCNCS using the GSRB Hamiltonian. $E(0,0)/hc = 42.6$ cm^{-1}.

K_a	$v_b = 0$	$v_b = 1$	$v_b = 2$	$v_b = 3$	$v_b = 4$	$v_b = 5$	$v_b = 6$
0	0.0	84.6	162.2	231.4	304.0	389.1	484.2
1	3.6	89.7	172.4	254.1	340.1	432.8	532.8
2	13.9	103.6	192.5	282.7	376.9	476.3	581.1
3	30.2	124.2	218.8	315.6	416.1	520.7	629.8
4	51.9	150.2	249.9	352.1	457.6	566.8	679.6
5	78.3	180.7	284.9	391.7	501.5	614.5	730.7
6	110.0	215.2	323.4	434.1	547.6	664.0	783.2
7	143.3	253.0	364.9	479.1	595.8	715.2	837.1
8	181.0	294.0	409.1	526.4	646.1	768.2	892.4
9	221.8	337.7	455.7	575.9	698.2	822.7	949.1

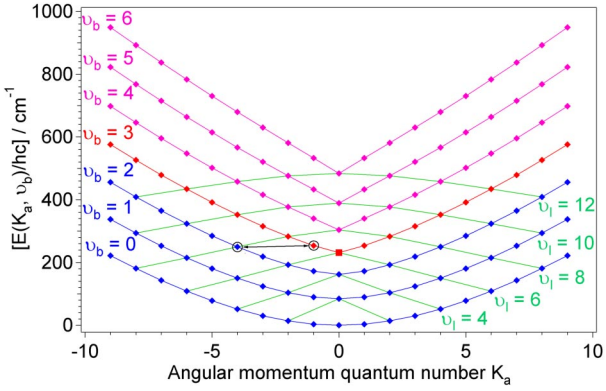

FIG. 3 (color online). Quantum monodromy plot of calculated v_b bending vibrational levels. The color scheme follows Fig. 2. A local Coriolis resonance is indicated between the two bending states $v_b = 2$, $K_a = 4^e$ and $v_b = 3$, $K_a = 1^e$.

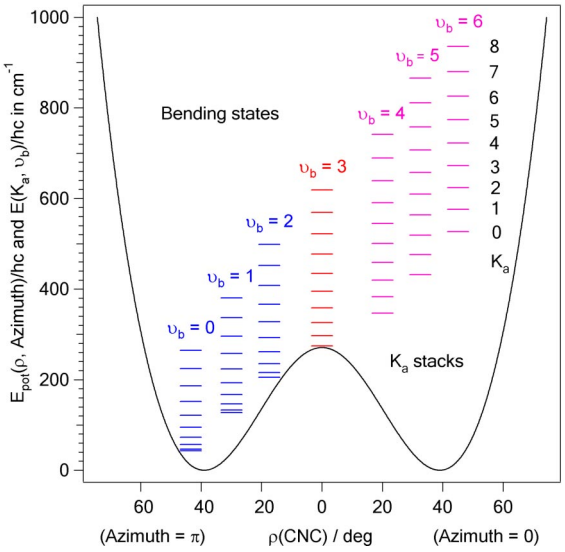

FIG. 4 (color online). Cut through the effective two-dimensional bending potential energy function $E_{\text{pot}}(\rho, \text{Azimuth})/hc$ of the mode $\nu_b \equiv \nu_7$ for NCNCS. The bending coordinate ρ(CNC) is defined as the supplement of the CNC bond angle. The vibrational term values $E(K_a, \upsilon_b)/hc$ are also entered.

onto any representation of the rovibrational energy versus K_a. A representation of the end-over-end rotational energy, as in Fig. 2, accentuates the anomalies observed in the basic monodromy plot of $E(K_a, \upsilon_b)$ versus K_a for NCNCS given in Fig. 3. Since the results we present here were first reported [14], Tennyson and coworkers [15] have managed to assign very highly excited levels in H_2O which exhibit energy-momentum characteristics similar to those shown here, also confirming the pattern imposed by quantum monodromy.

The first recognition that interesting minima can be seen by plotting rovibrational term values of a three-atomic molecule against K_a, as it passes from a bent to linear configuration, must be attributed to Dixon's NH_2 work [16]. The topological perspective has revealed further systematic properties of such systems. With our extension of this approach to the B_{eff} values, we believe that we have introduced, in addition, an aid for the assignment of the complex rotational structure in spectra of quasilinear molecules.

We thank J. Tennyson and M. Child for stimulating discussions. The experimental work at OSU is supported by the Army Research Office, and the GSRB work by the Natural Sciences and Engineering Research Council of Canada.

[1] L. M. Bates, J. App. Math. Phys. **42**, 837 (1991).
[2] M. S. Child, T. Weston, and J. Tennyson, Mol. Phys. **96**, 371 (1999).
[3] M. S. Child, J. Phys. A **31**, 657 (1998).
[4] M. S. Child, J. Mol. Spectrosc. **210**, 157 (2001).
[5] M. A. King, H. W. Kroto, and B. M. Landsberg, J. Mol. Spectrosc. **113**, 1 (1985).
[6] S. C. Ross, J. Mol. Spectrosc. **132**, 48 (1988).
[7] M. A. King and H. W. Kroto, J. Chem. Soc. Chem. Commun. **1980**, 606 (1980).
[8] I. Medvedev, M. Winnewisser, F. C. DeLucia, E. Herbst, E. Białkowska-Jaworska, L. Pszczółkolwski, and Z. Kisiel, J. Mol. Spectrosc. **228**, 314 (2004).
[9] I. R. Medvedev, M. Winnewisser, B. P. Winnewisser, F. C. DeLucia, and E. Herbst, J. Mol. Struct. **742**, 229 (2005).
[10] S. C. Ross, T. A. Cooper, S. Firth, H. W. Kroto, and D. R. Walton, J. Mol. Spectrosc. **152**, 152 (1992).
[11] H. Lichau, C. W. Gillies, J. Z. Gillies, S. C. Ross, B. P. Winnewisser, and M. Winnewisser, J. Phys. Chem. A **105**, 10 065 (2001).
[12] J. Koput, J. Mol. Spectrosc. **118**, 189 (1986).
[13] J. Koput, J. Mol. Spectrosc. **118**, 448 (1986).
[14] B. P. Winnewisser, M. Winnewisser, I. R. Medvedev, M. Behnke, F. C. DeLucia, S. Ross, and J. Koput, in *60th International Symposium on Molecular Spectroscopy, Columbus, OH, 2005*, Report No. TH07.
[15] N. F. Zobov, S. V. Shirin, O. L. Polyansky, J. Tennyson, P. F. Coheur, P. F. Bernath, M. Carleer, and R. Colin, Chem. Phys. Lett. (to be published).
[16] R. N. Dixon, Trans. Faraday Soc. **60**, 1363 (1964).